Elucidating the large variation in ion diffusivity of microelectronic packaging materials

Herrmann, A.; van Soestbergen, M.; Erich, S. J.F.; van der Ven, L. G.J.; Huinink, H. P.; van Driel, W. D.; Mavinkurve, A.; De Buyl, F.; Adan, O. C.G.

DOI
10.1016/j.microrel.2022.114656

Publication date
2022

Document Version
Final published version

Published in
Microelectronics Reliability

Microelectronics Reliability 136 (2022) 114656

Contents lists available at ScienceDirect

Microelectronics Reliability

journal homepage: www.elsevier.com/locate/microrel

Elucidating the large variation in ion diffusivity of microelectronic packaging materials

A. Herrmann [a,*], M. van Soestbergen [b], S.J.F. Erich [a,c], L.G.J. van der Ven [a], H.P. Huinink [a], W.D. van Driel [d,e], A. Mavinkurve [b], F. De Buyl [f], O.C.G. Adan [a,c]

[a] Dep. of Applied Physics, Eindhoven University of Technology, P.O. Box 513, 5600 MB Eindhoven, the Netherlands
[b] NXP Semiconductors, Gerstweg 2, Nijmegen 6534 AE, the Netherlands
[c] TNO, High Tech Campus 25, 5656 AE Eindhoven, the Netherlands
[d] Signify, High Tech Campus 7, 5656 AE Eindhoven, the Netherlands
[e] Delft University of Technology, EEMCS Faculty, Delft, the Netherlands
[f] Dow Silicones Belgium s.r.l, Industrial park – Zone C, 7180 Seneffe, Belgium

ARTICLE INFO

Keywords:
Ion diffusion
Microelectronic packaging
Mold compound
TOF-SIMS
Diffusion cell

ABSTRACT

The risk of corrosion poses a challenge to meet the stringent reliability requirements of microelectronic devices that are used in harsh environments. Microelectronic devices are often encapsulated in polymer packaging materials, which protect them from corrosion. These polymers are, however, not completely hermetic and thus allow small amounts of ions and moisture to reach the device, which might cause corrosion of the microelectronic circuitry. To improve and predict the reliability of the device, it is important to quantify the ion diffusivity in these materials. Previously reported values for the ion diffusivity vary by multiple orders of magnitude for a single class of material. Here, we investigate the causes for this discrepancy using three experimental methods: (i) saltwater immersion, (ii) diffusion cell measurements, and (iii) transient electric current measurements. Several materials, such as silicone, epoxy, and polyamide, were tested to cover the broad spectrum of polymers used by the microelectronics industry. We found that the discrepancies are likely due to the strong dependence of the ion diffusivity on both the moisture content within the polymers, as well as on the salt concentration and pH of the solutes. Furthermore, we found that the very low ion diffusivity causes long measuring times, and thus a large risk for errors from contamination, leakage, or minor defects in the samples.

1. Introduction

Fueled by both the increasing outdoor usage (e.g. handheld devices, and automotive applications), and the advancing technology (e.g. finer interconnect pitch, and smaller feature sizes), the reliability requirements for microelectronic products are becoming increasingly challenging to meet. Here, ion transport through polymer materials is an important topic, as it might cause failures such as corrosion of bond pads and wires [1–7], malfunction of the electric circuit due to charge accumulation on the die surface [8,9], or the growth of dendritic structures between leads [10–12]. The source of ionic contaminants can be intrinsic, e.g. residues of the synthesis of the material [13] or extrinsic, such as the 'cleaning flux' used for soldering [14]. Depending on the application and requirements, different polymers are used as a barrier against ionic attacks [15]. Even though they are chosen to be a strong barrier, they cannot fully prevent water and ion transport. Therefore, fundamental knowledge on both moisture and ion transport through polymers is essential for the design of reliable microelectronics.

While abundant work has been reported on moisture uptake of different packaging materials [16–19], literature on ion transport measurements is scarcer. Additionally, reported ion diffusion coefficients can differ by orders of magnitude, as summarized for Epoxy Mold Compound (EMC) in Table 1. Here the highest value is $1.2{\cdot}10^{-11}$ m^2/s [20], whereas the lowest value is $3.2{\cdot}10^{-21}$ m^2/s [21] at identical temperature. Considering the characteristic diffusion timescale, L^2/D, where L is the length of the diffusion path and D the diffusion coefficient, these values mean that the time for ions to cross 100 μm of material equals <10 min in the first case and over 100,000 years in the latter case. This large variation makes accurate reliability predictions based on ion transport virtually impossible.

* Corresponding author.
E-mail address: a.herrmann@tue.nl (A. Herrmann).

https://doi.org/10.1016/j.microrel.2022.114656
Received 24 January 2022; Received in revised form 1 July 2022; Accepted 14 July 2022
Available online 30 July 2022

In the current work, we analyze the cause for these variations and reflect on the best way to measure ion diffusivity in microelectronics packaging materials. For this we discuss three common methods: (i) saltwater immersion, (ii) diffusion cell measurements, and (iii) time-of-flight measurements upon electric field reversal. Using these methods, we tested several materials. The first material is EMC, which is commonly used as an encapsulant. Next, a thermo-set epoxy resin is used that finds its application as 'underfill' to glue the bottom of the micro-electronic package to the printed circuit board. Furthermore, silicone is studied. Silicones are used for several purposes in microelectronic packages, such as, die attach materials (i.e. glues), protection layers on the die surface, or as sealants for Micro-Electro-Mechanical Systems (MEMS) packaging. The silicones used in this work, however, are those used for Light-Emitting Diode (LED) packages. Finally, polyamide in the form of nylon will be investigated. This thermoplastic is used by system integrators to form a module body in which microelectronics devices are embedded. Furthermore, polyamides are used as scratch protection layers on wafers, and as dielectric material in redistribution layers for chip-scale packages.

The work is organized along the line of the three above-mentioned experimental methods, followed by a discussion section, where we combine the lessons learned from literature and our own research on how certain factors (e.g. pH, moisture, ion content, and temperature) influence the experiments.

2. Saltwater immersion

The principle of the saltwater immersion experiment is similar to the commonly used moisture uptake measurements. Namely, samples are immerged in a salt solution for a defined amount of time, after which the amount of ion uptake is determined as explained below. The values in Table 1 indicate that this method gives the lowest value for the diffusivity. In the current work we re-analyze the results of the saltwater immersion experiments reported in [27]. Here, the specimens were made of a biphenyl-based EMC ($T_g \sim 120$ °C, 90 *wt%* filler), which was molded onto Heatsink Very thin Quad-Flat No-leads (HVQFN) lead frames. After molding, the EMC was manually removed from the lead frames yielding 600 μm thick strips. These strips were cut into parts of 20 by 10 mm, which were immersed in demi-water for 96 h at 80 °C to remove any ionic contamination. Subsequently two sets of five strips were placed in separate beakers containing 200 ml demi-water at 30 °C and 60 °C. After equilibrating the specimens for 24 h, NaCl was added to obtain a 0.15 M solution. Specimens were taken out at different time intervals and were dried to remove any redundant solution from the surface. The specimens were then transferred into separate pressure vessels to extract all ions from the EMC. The vessel consists of a Polytetrafluoroethylene (PTFE) inner shell with a stainless-steel jacket containing 20 ml ultra-pure water. The extracts were finally analyzed using ion chromatography, and the amount of NaCl absorbed by the EMC was determined.

The results for the saltwater immersion experiments are presented in Fig. 1A. The ion concentration inside the material increases with time, showing a faster absorption at higher temperature. For the evaluation of the diffusion coefficient it is necessary to know the final (saturation) ion content, which remains ambiguous from the results of Fig. 1A. In ref. [27] a saturation limit of tens of ppm (mg of absorbed NaCl per kg mold compound) was assumed, which is of the same order of magnitude as the total amount of ions in commercial EMC. Fitting the data to Fick's law of diffusion using this saturation limit gives a diffusion coefficient in the order of 10^{-13} m^2/s [27], which is of the same order of magnitude as the diffusion coefficient for water in this material. However, when assuming that the ions need to be hydrated within the EMC (as for Nylon [28]), the maximum salt concentration might be estimated by the solubility of NaCl in water. Taking the product of the absorbed water in the mold compound (ref. [16]) and the solubility of NaCl in water yields a saturation limit of 450 and 650 ppm at 30 °C and 60 °C, respectively. For these values the salt sorption would still be in its initial stage, and is best plotted on a square root of time scale as shown in Fig. 1A. The diffusion coefficient follows from the slope of the fit, k, using $D = \pi(k \cdot L/4 \cdot m_{sat})^2$, where L is the thickness of the sample, and m_{sat} denotes the saturation level. This results in a diffusion coefficient for both temperatures of $7 \cdot 10^{-16}$ m^2/s, which is three orders of magnitude lower than assessed previously, and agrees with the previously reported observation that the diffusivity of ions is orders of magnitude lower than that of water in mold compounds [2].

In ref. [27] only the ion sorption data was reported. Later, time-of-flight secondary ion mass spectroscopy (TOF-SIMS) was used to further analyze the ion penetration into the EMC. For the TOF-SIMS analysis a sample was broken and the cleave analyzed. The measured intensity of sodium is shown in the inset of Fig. 1B (high intensity appears brightest). An approximately 10 μm thick layer of sodium is present on the surface of the sample. Although the cleave surface appeared smooth, a closer examination showed that it was quite rough, which reduces the accuracy of the analysis. Therefore, a depth profile from the surface of the sample is made, which is shown in the graph of Fig. 1B. The x-axis is roughly calibrated using the Na map from the previous analysis, whereas the y-axis is normalized to the highest intensity. The highest intensity for the salt-soaked sample is about 90 times higher than the (uniform) intensity of the non-immersed reference sample, which is in line with the assumption of the 450 ppm saturation limit for the immersion experiment. According to Fick's law, the normalized concentration scales with [29] $\mathrm{erfc}(x/(2 \cdot \sqrt{Dt}))$, where x is the distance away from the source and t is the elapsed time. Fitting this relation to the measured Na profile gives a diffusion coefficient of $5 \cdot 10^{-17}$ m^2/s, which is within an order of magnitude of the value determined from the data of Fig. 1A. Given the approximate nature of both experiments, we believe that this is a fair correlation.

Table 1
Literature values for the ion diffusion coefficient in epoxy mold compound at 85 °C.

D [m^2/s]	Method	EMC	Remarks	Ref.
$\sim 4 \cdot 10^{-16}$	Diffusion cell	Several samples T_g = 115–166 °C	pH = 10, for neutral and low pH no diffusivity detected	2
$\sim 5 \cdot 10^{-19}$	TOF-SIMS	77-87 *wt%* filler	Neutral solutions of NaCl at 0.15 M	2
$3.2 \cdot 10^{-21}$	DSIMS	Sumitomo 7351LS	Immersion in 2 M NaCl solutions	21
$3 \cdot 10^{-16}$ - $2 \cdot 10^{-18}$	SIMS	No info	85 % RH + drop of saturated NaCl on top of samples,	22
$\sim 4 \cdot 10^{-13}$	Diffusion cell	No info	100 ppm and 1 M NaCl (temperature not reported)	22
$1.2 \cdot 10^{-11}$	Diffusion cell	No info	1 M KCl solution, 3× higher value for pH = 11 and 3	20
$6.4 \cdot 10^{-15}$	Diffusion cell	No info	'concentrated' KCl solution, and 30 V electric bias	23
$6.9 \cdot 10^{-15}$	Diffusion cell	No info	'concentrated' KCl solution, and 47.5 V/m electric field	24
$6.9 \cdot 10^{-15}$	Diffusion cell	No info	Experiments at 1 M KCl	25
$\sim 4.6 \cdot 10^{-19}$ (extrapolated)	Electrochemical Impedance Spectroscopy	T_g = 132 & 162 °C; 80-88 *wt%* filler;	Dry experiment at high temperature. Na^+ diffusion from amalgam electrode	26

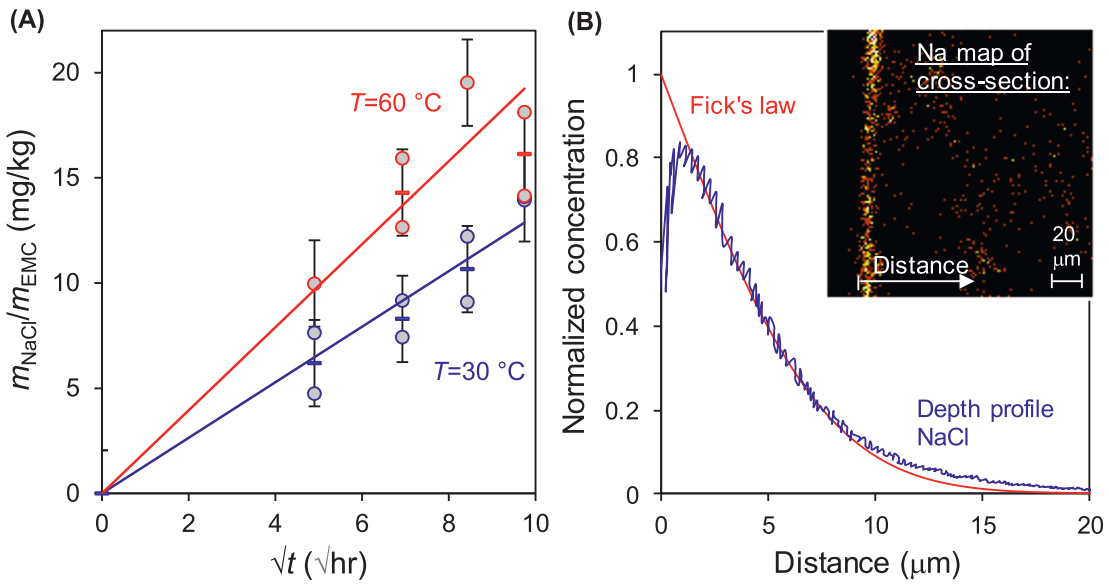

Fig. 1. Results of the immersion experiments of mold compound immerged in 0.15 M NaCl. (A) Absorbed ions as a function of time; the symbols indicate the measured data, the error bars represent three times the standard deviation of all data points, the full lines are linear fits. (B) TOF-SIMS Na depth profile and corresponding fit to Fick's law. The inset gives the Na map of the sample's cross-section.

3. Diffusion cell

3.1. Experimental setup

The setup consists of a sample that is mounted between a donor and a receptor cell (see Fig. 2). The donor cell contains the solvent and solute, while the receptor cell contains only the solvent. Due to the concentration difference, the solute diffuses through the sample into the receptor cell, where the solute concentration is measured [30,31]. This diffusion process can be divided into two phases by assuming negligible intrinsic ion contamination within the sample. In the first phase, the ions permeate through the sample, so that no ions have reached the receptor cell yet. The length of this phase is defined by the time lag parameter; $t_{lag} = L^2/6D$ [31]. The second phase starts when the ions reach the receptor cell. For ideal cells (where the solute concentration remains constant and the concentration in the receptor cell is much less than the solute concentration throughout the experiment), the flux through the sample remains constant during this phase. The amount of ions Q in the receptor cell is given by [31],

$$Q = \frac{A\,D\,C_0}{L}\left(t - t_{lag}\right), \tag{1}$$

where A is the exposed sample area, C_0 is the concentration absorbed in the surface of the sample on the donor side, L the sample thickness, t is time, and D is the diffusion coefficient of the salt (not of the individual ions). Based on charge neutrality the following relation can be found for the diffusion coefficient of a binary electrolyte [32],

$$D = \frac{D_c D_a (z_c - z_a)}{z_c D_c - z_a D_a}, \tag{2}$$

where z is the valence of the ions, and subscript c and a denote the positive cations, and negative anions, respectively.

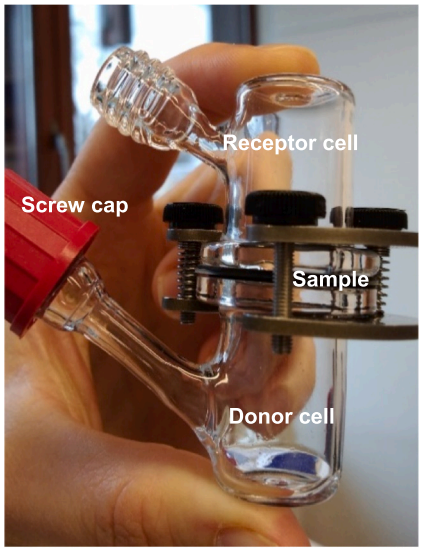

- Moisture evaporation from the cells was prevented by using screw caps instead of press-on lids.
- Samples were thoroughly checked on micro-voids that can pass ions directly.
- The glass cells were glued to the sample to prevent salt from creeping along the gaskets from the donor to receptor cell directly. Silicone glue was used for elevated temperatures, whereas bees wax turned out as the best solution at room temperature.
- All sealing materials were checked for ion impurities, preventing ion contamination during the experiment.
- To release the pressure in the cells that builds up at elevated temperature the screw caps were loosened during each temperature change.

Fig. 2. The photo shows the diffusion cell, where ions from the donor cell diffuse through the sample and reach the receptor cell. The text box shows measures that were taken to achieve a robust method.

As we expect slow transport, and thus low solute concentrations, a small volume of the receptor cell is needed to reach the detection limit in a reasonable amount of time, while a sufficiently large volume is needed for analysis of the solute concentration. For our experiment we chose cells with a receptor volume of $V = 7$ ml. A photo of the diffusion cell is shown in Fig. 2. At the end of the sampling interval, the whole receptor volume was emptied and filled with fresh ultrapure water. The sampling intervals need to be long enough to reach a concentration above the detection limit C_{lim}. The minimum diffusion coefficient that can be measured with a sampling interval t_s follows from eq. (1). In steady state, the first term of the equation applies. With the relation $Q = CV$, we get

$$D_{min} = \frac{C_{lim}\, V\, L}{A\, C_0\, t_s}. \tag{3}$$

In this work, the concentration of potassium and chloride ions was measured by ion chromatography (using the ICS-90 Dionex chromatograph with a DS5 electrochemical detector). With a 100 µl injection loop, we obtain a detection limit of $5{\cdot}10^{-8}$ M for potassium ions, which gives a D_{min} in the order of 10^{-19} m^2/s for realistic values of t_s.

We have performed measurements on (i) two optical silicones with glass transition temperatures of 30 and 50 °C (same materials as in ref. [33]), and sample thickness of 120 and 150 µm, respectively, (ii) an unfilled epoxy ($T_g = 115$ °C) produced from epoxy Novolac compound EPN1180 with Bisphenol A as hardener and triphenylphosphine as catalyst (same as in ref. [34]), and a sample thickness of 390 µm, and (iii) polyamide-6 with a ~22 % degree of crystallinity, a melting point of 220 °C (as in ref. [28,35]), and a sample thickness of 60 µm. The whole setup was placed in an oven to determine the diffusion coefficient at elevated temperatures up to 90 °C. The measures that were taken to achieve a stable and robust method are listed in the text box of Fig. 2. All samples were measured using a 1 M KCl solution in the donor cell.

3.2. Validation of the diffusion cell

To validate the diffusion cell, we additionally measured Mn^{2+} transport through the nylon samples using a 1 M $MnCl_2$ solution at room temperature and compared it with the NMR (nuclear magnetic resonance) results of ref. [28]. To stabilize the $MnCl_2$ solution, HCl was added to prevent Mn^{2+} to react with CO_2, which resulted in a pH of ~3 in the donor cell. The Mn^{2+} concentration was determined using UV-VIS spectroscopy. The Mn^{2+} ions were oxidized to MnO_4^- by adding KIO_4 was as the reagent, and acid was used to stabilize the manganese in the right oxidation state [36,37]. MnO_4^- has an absorption peak at a wavelength of 535 nm. A fit of the accumulated amount of Mn^{2+} in the receptor cell as a function of time to Eq. (1) is given in Fig. 3A. The fit is very sensitive to the concentration of $MnCl_2$ absorbed in the surface of the sample, C_0. Theoretically it is possible to obtain the diffusion coefficient without knowing C_0 from the lag time by determining the intercept for $Q = 0$. However, the intercept could not be accurately determined. Therefore, we used the data published in ref. [28], where for 1 M $MnCl_2$ it was found that C_0 equals ~60 mM. Consequently, the diffusion coefficient for $MnCl_2$ equals $2.6{\cdot}10^{-14}$ m^2/s, which compares favorably with the reported value of $3{\cdot}10^{-14}$ m^2/s in ref. [28].

3.3. Dependence of diffusion speed on permeant size

When comparing the concentrations of the Mn^{2+} and Cl^- ions, we found the measured Cl^- concentration to be up to 9 times the Mn^{2+} concentration. Based on charge neutrality however, the chloride concentration is expected to be two times higher than the Mn^{2+} concentration. At the same time, the pH in the receiving cell was lowered to below neutral. This suggest that the additional chloride in the receptor cell is the result of HCl diffusion. The surplus of chloride passing through the sample (i.e. the measured amount of chloride minus two times the measured manganese amount) is plotted in Fig. 3(A). The rate of refreshing the $MnCl_2$ solution was chosen to ensure a constant Mn^{2+} concentration, but this was too low to ensure a constant HCl concentration in the donor cell. Each third data point (just prior to refreshing the $MnCl_2$ solution), the Cl^- accumulation in the receiving cell was found to be significantly lower than in the preceding two time intervals. Therefore, these data points are discarded. The resulting data are well described using a diffusion coefficient of $1.35{\cdot}10^{-13}$ m^2/s. For this evaluation we estimate C_0 to be 45 mol/m^3, which is the average of the values for Mn^{2+} [28] and K^+ [35].

In case of KCl diffusion through nylon, the measured chloride concentrations were identical to the potassium concentrations for all measurements. Here the absorbed K^+ concentration was assumed to be 30 mol/m^3 [35], which gives a fitted diffusion coefficient of $1{\cdot}10^{-13}$ m^2/s for KCl, which is higher than the value found for $MnCl_2$. To determine the effect of the permeant size, we compute the diffusion coefficients of the individual ions. Since the hydrated radii of K^+ and Cl^- are near identical [38], we assume that $D_{K+} = D_{Cl-} = D_{KCl}$. Consequently, we use

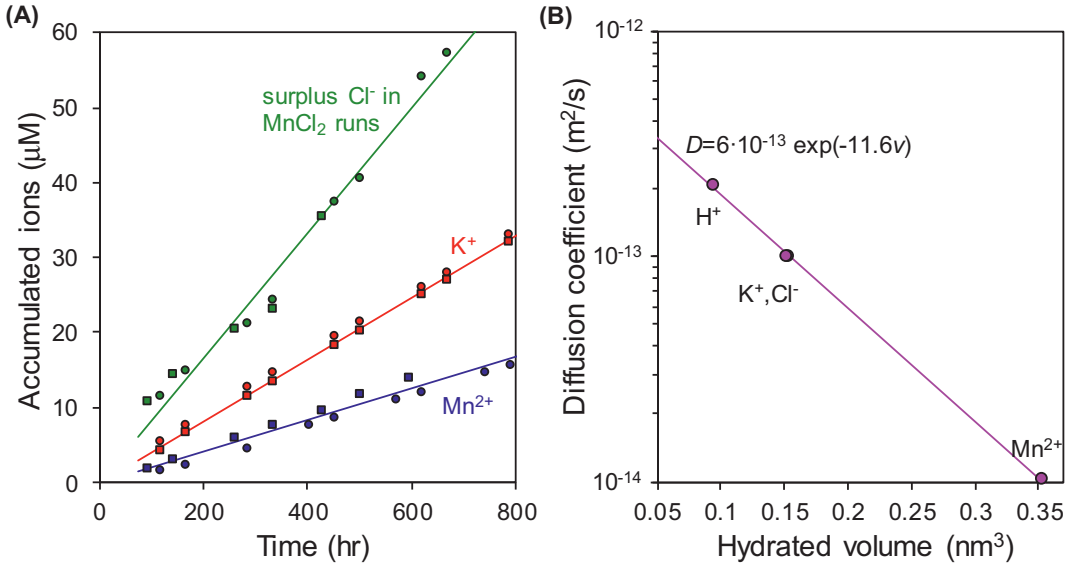

Fig. 3. Results for the diffusion cell measurement on Nylon 6 at room temperature. (A) Accumulated amount of ions which permeated through the film at either 1 M KCl or 1 M $MnCl_2$ in the donor cell. (B) The estimated diffusion coefficients plotted as a function of the hydrated ion volume (v).

Eq. (2) to compute the diffusion coefficients for H^+ and Mn^{2+} from the diffusion coefficient of their ion pairs, i.e., HCl = $1.35{\cdot}10^{-13}$ m^2/s and $MnCl_2$ = $2.6{\cdot}10^{-14}$ m^2/s, respectively. This yields $D_H = 2.1{\cdot}10^{-13}$ m^2/s and $D_{Mn} = 1{\cdot}10^{-14}$ m^2/s. The values for the individual ions are plotted in Fig. 3B as a function of the hydrated ion volume. The solid line represents a fit given by $D = 1{\cdot}10^{-13}\exp(-11.6v)$, with v the hydrated ion volume in nm^3, which indicates an exponential relation between the diffusion coefficient and the size of the permeant [39].

3.4. Diffusion cell measurements in epoxy and optical silicones

For the epoxy and optical silicones no ions passed through the samples to the receptor cell after 32 and 114 days, respectively, which is in line with ref. [2]. Even at elevated temperatures up to 90 °C no ions passed though the samples. Therefore, the values for epoxy and silicone are estimated using Eq. (3). The actual values, however, might be orders of magnitude lower. The values of the experiments are listed in Table 2.

4. Time-of-flight upon electric field reversal

Ion transport driven by an electric field can reduce the measuring times significantly compared to concentration driven approaches. The applied electric field lowers the barrier height for diffusive jumps between adjacent sites in one direction, and at the same time increases the barrier height for jumps in the opposite direction, thus increasing ionic conduction through the material [40]. However, applying a constant electric field and recording the corresponding electric current might result in unstable readings for the conductivity due to charging of the system, which causes transient electric currents [41]. Furthermore, it will be unclear if the current is partly carried by electrons as well. If only ions carry the current, then the conductivity of a material is given by [32],

$$\sigma = \frac{F^2}{RT}\sum_i z_i\, C_i\, D_i, \tag{4}$$

where F is the Faraday constant, R is the gas constant, T is the temperature, and C_i denotes the concentration of ionic species i and z_i is the corresponding valence. When determining the diffusion coefficient using this approach, it is necessary to know the ion content in the material [42].

The necessity for knowing the ion content in the material can be circumvented by measuring the time-of-flight of the ions upon reversal of the electric field [43,44]. Kohn et al. [45] demonstrated this technique on 20–70 μm thick layers of poly(methylmethacrylate) where lithiumtriflate salt was added. In the current work we use an underfill material, with a glass transition temperature of ~120 °C, and ~85 ppm intrinsic chloride concentration. The underfill was cured in a silicone mold at conditions as specified by the supplier. The lateral dimensions of the specimen are 60 × 40 mm, with a thickness of ~600 μm. Two adhesive aluminum foil electrodes were used to cover the surface almost completely. The electric current was recorded at 100 Volt potential difference using a Keithley 617 electrometer. The samples were placed in an oven to control the temperature and to provide electromagnetic shielding.

A typical measurement cycle is given in Fig. 4A. In the first part of the cycle, the current rapidly decays as the bulk of the material will become depleted of ions until a steady-state current is reached, which is believed to be dominated by electrons hopping through the polymer matrix. Once the bulk is sufficiently depleted, the potential is reversed, and the ions flow back into the bulk, which will lead to an increase in conductivity. This increase continues until the ions reach the opposite electrode, leading to a peak in measured current at the transit time, after which the depletion starts again. From the transit time t_p, the ion diffusion coefficient is computed using [43–46],

$$D = \frac{RT}{F}\frac{L^2}{2t_p\Delta V}, \tag{5}$$

where L is the sample thickness and ΔV the applied potential difference between the electrodes.

As the temperature decreases, the transit time becomes less visible until it becomes indistinctive at temperatures below 90 °C. In Fig. 4B the computed diffusion coefficient is plotted as a function of temperature. It follows an Arrhenius behavior with and activation energy of 69.4 kJ/mol (=0.72 eV). For EMC the transit time could not be observed, not even for temperatures well above glass transition. We believe this is the result of the electric current being dominated by electron hopping [2].

5. Discussion

5.1. Effect of pH

A pH dependency in the ion diffusion coefficients in EMCs was reported in the literature, with significantly faster diffusion at both high and low pH compared to the neutral solutions (see Table 1). Lantz et al. [2] suggest that the epoxy might hydrolyze in basic environments and even observed a discoloration in their sample. A change in ion diffusivity accompanying a change in pH can in some polymers be due to ionization of the functional groups in the polymer (e.g. carboxyl and amino groups are known for this effect [47] but are not expected in EMCs).

In this work we found that protons (H^+) might replace the larger Mn^{2+} cation as counter ions, enhancing the transport of Cl^- in our diffusion cell measurements on polyamide, as we observed that the diffusion speed of the ions was dependent on their hydrated radius (see Fig. 3). In the light of reports on the release of H_3O^+ in the hydrolyzation of non-cured parts of the EMC upon exposure to moisture [48,49], this result is also relevant for EMCs.

5.2. Effect of moisture

Moisture sensitivity is one of the likely reasons why the reported values for the ion diffusivity vary significantly. Cornigli et al. [50] studied the space charge distribution in EMC by pulsed electro acoustic analysis and observed an accumulation of negative charge at the anode in wet EMC, but not in dry EMC, which indicates increased ion transport in wet EMC.

Ion diffusion studies in polyamide [28]. showed that water molecules facilitate the absorption and transport of ions into the polymer by plasticizing the polymer matrix and participating in the ion's hydration

Table 2
Measured diffusion cell results for different materials.

Material	Thickness [μm]	Remark	D [10^{-14} m^2/s]
Epoxy (unfilled)	390	1 M KCl solution, No ions detected in 32 days, sampling interval 3–4 days, temperature ranged from 40 to 90 °C during experiment	<0.9
Silicone	120 & 150	1 M KCl solution, No ions detected after 114 days, 10–14 days sample interval, temperature range 40–90 °C	<0.025
Nylon	60	1 M $MnCl_2$ (pH = 3), room temperature, up to 9× higher Cl^- concentration found	2.6 ± 0.2
		1 M KCl solution at room temperature $D_{K+} = D_{Cl-}$ for all measurements	10

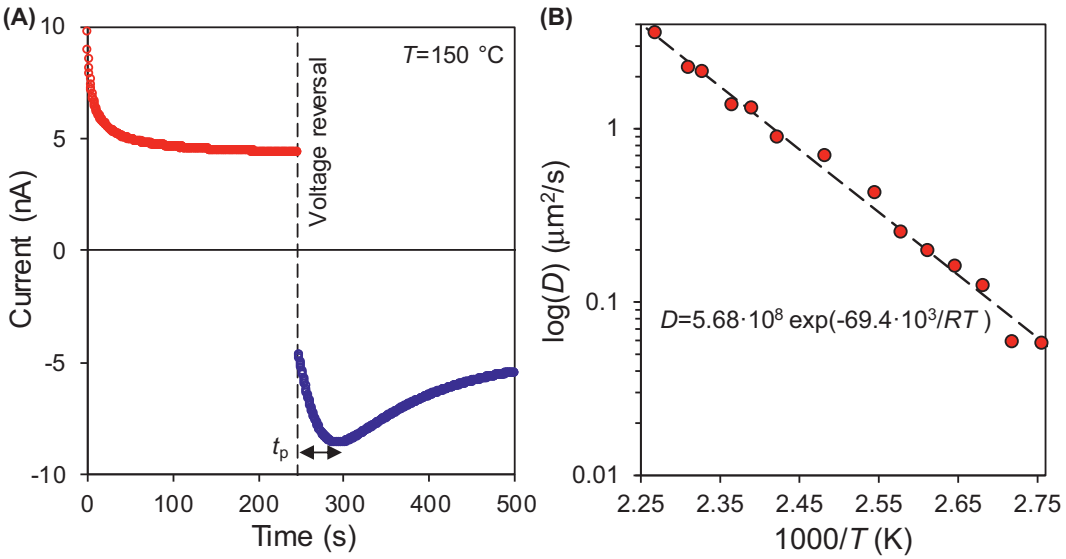

Fig. 4. Results for the time-of-flight experiments. (A) Example of the recorded electric. (B) The computed diffusion coefficient as a function of temperature, the dashed line gives an Arrhenius fit.

shell. The absorption of water from solution was shown to precede the ion absorption and transport through the polymer. It is thus expected to see faster ion transport in samples that were pre-soaked than in samples which first have to absorb moisture. For comparison of experimental results, it is therefore necessary to report the preconditioning procedure of the samples.

5.3. Salt concentration of the solute

An example of a salt concentration effect is the data reported by Lantz and co-workers [2,21]. The immersions measurement with 0.15 M NaCl solution gave two orders of magnitude higher diffusion coefficients than the measurement with a 2 M solution, which might be explained by the water activity of the solution. The water activity in a 0.15 M NaCl solution is >0.99, while it is ~0.93 for a 2 M solution [51]. This difference leads to a higher moisture content in the sample for the lower NaCl concentration and may explain the higher diffusivity found. For both immersion and diffusion cell experiments, moisture concentrations can be tuned by changing the salt concentration in solution. Additionally, it was demonstrated in Nylon that water from concentrated solutions enters the polymer much slower than water from diluted solutions [35]. This effect might also play a role in other polymers.

5.4. Glass transition

The time-of-flight measurements show that above glass transition, the temperature dependence of the ion diffusion coefficient is given by the Arrhenius relation. The distinct peak of the transit time, however, vanished rapidly for temperatures below glass transition, which seems appropriate as above glass transition the segmental motion leads to an increase of free volume, facilitating ion transport [40]. It is reasonable that well below glass transition the diffusion coefficient does not longer follow the Arrhenius fit of Fig. 4, as e.g. suggested by the conductivity data in ref. [40,42].

6. Conclusions

The presented experimental methods, as well as the discrepancies in literature values, show that measuring the ion diffusivity in microelectronic packaging materials is complex. The measurements are strongly influenced by factors such as the moisture content, ion concentration, pH, electric bias, and temperature. Furthermore, the diffusion coefficient for most polymer materials are very low, and thus require prolonged experiments. In this work we have shown that diffusion cell experiments might not even provide results due to the slow transport. The experimental time can be drastically reduced by using very thin samples (e.g. <50 µm), but fabricating such thin samples is often not possible due the size of the filler particles. Moreover, there are many factors which can cause errors in a diffusion cell experiment. This might be a reason for the high literature values for the diffusion coefficients of ions in epoxy mold compounds obtained using diffusion cells, which do not match values obtained with other techniques. Experimental times can also be significantly reduced by using the method of time-of-flight upon electric field reversal. However, these experiments only gave results for temperatures above glass transition, and only appear to work for materials where the ionic conduction is large compared to the electron conduction. Presumably the best method for measuring ion transport in packaging materials is a soaking experiment combined with a TOF-SIMS analysis. Here measuring times are significantly shorter than for the diffusion cell experiment as ions do not need to travel through the entire thickness of the sample.

In future work, saltwater immersion experiments using low-concentrated ion solutions combined with TOF-SIMS analysis can be a starting point in characterizing ion transport in a worst-case scenario of a wet packaging material. This method might also be used to further characterize the effect of pH on Cl^- diffusivity. As ion diffusion is highly dependent on moisture content, further methods allowing for a humidity control of the material during experiments (not relying on altering the salt concentration) need to be investigated to gain a realistic perspective on the ion diffusion speed in a final product.

CRediT authorship contribution statement

A. Herrmann Conceptualization, Investigation, Formal analysis, Writing - Original Draft, Writing - Review & Editing.

M. van Soestbergen Investigation, Formal analysis, Writing - Original Draft, Writing - Review & Editing.

S.J.F. Erich Conceptualization, Supervision, Writing - Review & Editing, Funding acquisition.

L.G.J. van der Ven Supervision.

H.P. Huinink, Writing - Review & Editing.

W.D. van Driel Resources, Writing - Review & Editing.

A. Mavinkurve Resources, Writing - Review & Editing.

F. De Buyl Resources, Writing - Review & Editing.

O.C.G. Adan Supervision, Writing - Review & Editing, Funding acquisition.

Declaration of competing interest

The authors declare that they have no known competing financial interests or personal relationships that could have appeared to influence the work reported in this paper.

Acknowledgments

The authors would like to thank NWO-TTW for their financial support, Huntsman for supplying the araldite resin and Dow Silicones for supplying the silicone resins. Funded by the Netherlands Organisation for Scientific Research (NWO): 13893.

References

[1] H.Y. Ueng, C.Y. Liu, The aluminum bond-pad corrosion in small outline packaged devices, Mater. Chem. Phys. 48 (1) (1997) 27–35.
[2] L. Lantz, M.G. Pecht, Ion transport in encapsulants used in microcircuit packaging, IEEE Trans. Compon. Packag. Technol. 26 (1) (2003) 199–205.
[3] M. Van Soestbergen, A. Mavinkurve, R.T.H. Rongen, K.M.B. Jansen, L.J. Ernst, G. Q. Zhang, Theory of aluminum metallization corrosion in microelectronics, Electrochim. Acta 55 (19) (2010) 5459–5469.
[4] X.J. Fan, E. Suhir, in: Moisture Sensitivity of Plastic Packages of IC Devices, Springer US, Boston, MA, 2010, pp. 503–522.
[5] M. Maeda, H. Seki, Study of EMC for Cu bonding wire application, in: 2013 14th International Conference on Electronic Packaging Technology, 2013, pp. 393–395.
[6] W. Bisheng, Comparison of Cl effect on Au-Al and Cu-Al HTS and bHAST wire bond reliability performance, in: 2019 IEEE 26th International Symposium on Physical and Failure Analysis of Integrated Circuits (IPFA), 2019, pp. 1–6.
[7] G.I. Ashok Kumar, A. Lambert, J. Caperton, M. Asokan, W. Yi, O. Chyan, Comparative study of chloride and fluoride induced aluminum pad corrosion in wire-bonded device packaging assembly, Corros. Mater. Degrad. 2 (3) (2021) 447–460.
[8] M. van Soestbergen, P.M. Biesheuvel, R.T.H. Rongen, L.J. Ernst, G.Q. Zhang, Modified poisson-nernst-planck theory for ion transport in polymeric electrolytes, J. Electrost. 66 (11–12) (2008) 567–573.
[9] I. Imperiale, et al., Role of encapsulation formulation on charge transport phenomena and HV device instability, Proc. - Electron. Compon. Technol. Conf. 2015-July (2015) 159–167.
[10] M. Pecht, Y. Deng, Electronic device encapsulation using red phosphorus flame retardants, Microelectron. Reliab. 46 (1) (2006) 53–62.
[11] S. Yang, J. Wu, A. Christou, Initial stage of silver electrochemical migration degradation, Microelectron. Reliab. 46 (9–11) (2006) 1915–1921.
[12] J. Park, Y.B. Jo, J.K. Park, G.R. Kim, Propensity of copper dendrite growth on subassembly package components used in quad flat package, IEEE Trans. Device Mater. Reliab. 8 (2) (2008) 368–374.
[13] R.C. Olberg, The effects of epoxy encapsulant composition on semiconductor device stability, J. Electrochem. Soc. 118 (1) (1971) 129.
[14] C.F. Dunn, J.W. McPherson, Recent observations on VLSI bond pad corrosion kinetics, J. Electrochem. Soc. 135 (3) (1988) 661–665.
[15] H. Ardebili, M.G. Pecht, Plastic encapsulant materials, Encapsulation Technol. Electron. Appl. (2009) 47–127.
[16] M. van Soestbergen, A. Mavinkurve, Anomalous water absorption by microelectronic encapsulants due to hygrothermal-induced degradation, J. Appl. Polym. Sci. 131 (24) (Dec. 2014).
[17] K.M.B. Jansen, M.F. Zhang, L.J. Ernst, D.K. Vu, L. Weiss, Effect of temperature and humidity on moisture diffusion in an epoxy moulding compound material, Microelectron. Reliab. 107 (November 2019) (2020) 0–5.
[18] E.H. Wong, R. Rajoo, Moisture absorption and diffusion characterisation of packaging materials - advanced treatment, Microelectron. Reliab. 43 (12) (2003) 2087–2096.
[19] J. Comyn, F. De Buyl, Mobility of water and alcohols in a silica reinforced siloxane network, Eur. Polym. J. 37 (12) (2001) 2385–2391.
[20] P. Lall, Y. Luo, L. Nguyen, Multiphysics model for chlorine-ion related corrosion in Cu-Al wirebond microelectronics packages, in: Proc. ASME 2015 Int. Mech. Eng. Congr. Expo, 2015.
[21] L. Lantz, M.G. Pecht, M. Wood, The measurement of ion diffusion in epoxy molding compounds by dynamic secondary ion mass spectroscopy, IEEE Trans. Compon. Packag. Technol. 31 (3) (2008) 527–535.
[22] V. Mathew, E. Wikramanayake, S.F. Chopin, Corrosion of copper wire bonded packages by chlorine containing foreign particles, in: 2020 IEEE 70th Electronic Components and Technology Conference (ECTC) vol. 2020-June, 2020, pp. 504–511.
[23] P. Lall, Y. Luo, L. Nguyen, Numerical multiphysics model for cu-al wire bond corrosion subjected to highly-accelerated stress test, Proc. - Electron. Compon. Technol. Conf. 2018-May (2018) 1628–1638.
[24] P. Lall, Y. Luo, S. Deshpande, L. Nguyen, Measurement of ion-mobility in copper-aluminum wirebond electronics under operation at high voltage and high temperature, in: ASME 2017 International Technical Conference and Exhibition on Packaging and Integration of Electronic and Photonic Microsystems, 2017, pp. 1–7.
[25] P. Lall, Y. Luo, L. Nguyen, Package-level multiphysics simulation of Cu-Al WB corrosion under high temperature/humidity environmental conditions, in: 2017 16th IEEE Intersociety Conference on Thermal and Thermomechanical Phenomena in Electronic Systems, 2017, pp. 1176–1184.
[26] S. Schwab, et al., Measuring sodium migration in mold compounds using a sodium amalgam electrode as an infinite source, Proc. Electron. Comp. Technol. Conf. (2017) 1159–1164.
[27] M.Van Soestbergen, L.J. Ernst, G.Q. Zhang, R.T.H. Rongen, Transport of corrosive constituents in epoxy moulding compounds, in: EuroSime 2007 Int. Conf. Therm. Mech. Multi-Physics Simul. Exp. Microelectron. Micro-Systems, 2007, 2007, pp. 4–8.
[28] N.J.W. Reuvers, H.P. Huinink, H.R. Fischer, O.C.G. Adan, Migration of divalent ions in nylon 6 films, Polymer (Guildf) 55 (8) (2014) 2051–2058.
[29] J. Crank, in: The Mathematics of Diffusion, 1975, pp. 11–27.
[30] H.A. Daynes, The process of diffusion through a rubber membrane, Proc. R. Soc. London. Ser. A 97 (685) (1920) 286–307.
[31] S.W. Rutherford, D.D. Do, Review of time lag permeation technique as a method for characterisation of porous media and membranes, Adsorption 3 (4) (1997) 283–312.
[32] J.S. Newman, in: Electrochemical Systems, Prentice-Hall, 1973, p. 229.
[33] A. Herrmann, et al., The influence of phosphor particles on the water transport in optical silicones for LEDs, Opt. Mater. 6 (X) (2020), 100047.
[34] X. Ma, K.M.B. Jansen, G.Q. Zhang, L.J. Ernst, Filler contents effects on the moisture absorption and viscoelasticity of thermosetting IC packaging polymers, in: 2006 7th Int. Conf. Electron. Packag. Technol. ICEPT '06, 2006, pp. 6–10.
[35] N.J.W. Reuvers, H.P. Huinink, H.R. Fischer, O.C.G. Adan, The influence of ions on water transport in nylon 6 films, Polymer (Guildf) 54 (20) (2013) 5419–5428.
[36] A. Shokrollahi, N. Shokrollahi, Determination of mn 2+ ion by solution scanometry as a new, simple and inexpensive method, Quim Nova 37 (10) (2014) 1589–1593.
[37] S.M. College, Measuring Manganese Concentration Using Spectrophotometry (Experiment), Santa Monica College, 2020.
[38] E.R. Nightingale, Phenomenological theory of ion solvation. Effective radii of hydrated ions, J. Phys. Chem. 63 (9) (1959) 1381–1387.
[39] M.H. Cohen, D. Turnbull, Molecular transport in liquids and glasses, J. Chem. Phys. 31 (5) (1959) 1164–1169.
[40] D. Cornigli, et al., Characterization of dielectric properties and conductivity in encapsulation materials with high insulating filler contents, IEEE Trans. Dielectr. Electr. Insul. 25 (6) (2018) 2421–2428.
[41] J. Vanderschueren, A. Linkens, Nature of transient currents in polymers, J. Appl. Phys. 49 (7) (1978) 4195–4205.
[42] W. Schuddeboom, M. Wübbenhorst, Question marks to the extrapolation to lower temperatures in high temperature storage life (HTSL) testing in plastic encapsulated IC'S, Microelectron. Reliab. 36 (11–12 SPEC. ISS) (1996) 1935–1938.
[43] J. Ulański, K. Friedrich, G. Boiteux, G. Seytre, Evolution of ion mobility in cured epoxy-amine system as determined by time-of-flight method, J. Appl. Polym. Sci. 65 (6) (1997) 1143–1150.
[44] K. Friedrich, J. Ulanski, G. Boiteux, G. Seytre, Time-of-flight ion mobility measurements in epoxy-amine systems during curing, IEEE Trans. Dielectr. Electr. Insul. 8 (3) (2001) 572–576.
[45] P. Kohn, K. Schr??ter, T. Thurn-Albrecht, Determining the mobility of ions by transient current measurements at high voltages, Phys. Rev. Lett. 99 (8) (2007) 1–4.
[46] R.E. Barker, Mobility and conductivity of ions in and into polymeric solids, Pure Appl. Chem. 46 (2–4) (1976) 157–170.
[47] M. Elimelech, W.H. Chen, J.J. Waypa, Measuring the zeta (electrokinetic) potential of reverse osmosis membranes by a streaming potential analyzer, Desalination 95 (3) (1994) 269–286.
[48] G. Lubineau, A. Sulaimani, J. El Yagoubi, M. Mulle, J. Verdu, Hysteresis in the relation between moisture uptake and electrical conductivity in neat epoxy, Polym. Degrad. Stab. 141 (2017) 54–57.
[49] W. Ahn, et al., Effects of filler configuration and moisture on dissipation factor and critical electric field of epoxy composites for HV-ICs encapsulation, IEEE Trans. Compon. Packag. Manuf. Technol. 10 (9) (2020) 1534–1541.
[50] D. Cornigli, et al., Electrical characterization of epoxy-based molding compounds for next generation HV ICs in presence of moisture, Microelectron. Reliab. 88–90 (2018) 752–755.
[51] A.J. Fontana, B: water activity of unsaturated salt solutions at 25°C, Water Act. Foods (2020) 557–559.